Line FRAP with the Confocal Laser Scanning Microscope for Diffusion Measurements in Small Regions of 3-D Samples

Kevin Braeckmans, Katrien Remaut, Roosmarijn E. Vandenbroucke, Bart Lucas, Stefaan C. De Smedt, and Joseph Demeester
Laboratory General Biochemistry and Physical Pharmacy, Ghent University, Ghent, Belgium

ABSTRACT We present a truly quantitative fluorescence recovery after photobleaching (FRAP) model for use with the confocal laser scanning microscope based on the photobleaching of a long line segment. The line FRAP method is developed to complement the disk FRAP method reported before. Although being more subject to the influence of noise, the line FRAP model has the advantage of a smaller bleach region, thus allowing for faster and more localized measurements of the diffusion coefficient and mobile fraction. The line FRAP model is also very well suited to examine directly the influence of the bleaching power on the effective bleaching resolution. We present the outline of the mathematical derivation, leading to a final analytical expression to calculate the fluorescence recovery. We examine the influence of the confocal aperture and the bleaching power on the measured diffusion coefficient to find the optimal experimental conditions for the line FRAP method. This will be done for R-phycoerythrin and FITC-dextrans of various molecular weights. The ability of the line FRAP method to measure correctly absolute diffusion coefficients in three-dimensional samples will be evaluated as well. Finally we show the application of the method to the simultaneous measurement of free green fluorescent protein diffusion in the cytoplasm and nucleus of living A549 cells.

INTRODUCTION

Fluorescence recover after photobleaching (FRAP) is a well-known fluorescence microscopy method for studying the mobility of molecules and nanoparticles on the microscopic scale (1,2). Since its conception in 1974 by Peters et al. (3) it has found widespread application in the biophysical, biological, pharmaceutical, medical, and material sciences. For example, FRAP has been used to study the translational mobility of all kinds of molecules in the cytoplasm of cells (4–8), nuclei of cells (5–7,9–11), and membranes (12–15). FRAP has also been used to study the mobility of macromolecules in extracellular matrices (1,16–20) and pharmaceutical solutions and gels (21-27).

In a FRAP experiment, a powerful light beam is used to irreversibly photobleach the fluorescent molecules in a micron-sized area of the sample. After photobleaching, photobleached molecules will gradually move out of the photobleached area and are replaced by unbleached molecules from the surroundings. Due to this diffusional exchange, the fluorescence inside the photobleached area will recover as a function of time and can be monitored by a highly attenuated light beam. Analysis of the recovery dynamics with an appropriate physical model yields information about the local effective diffusion coefficient and the fraction of mobile fluorescent molecules inside the bleach area (23).

During the first two decades since its introduction, FRAP was mainly based on the photobleaching by a stationary light beam focused by the microscope objective lens to a small spot (28–33). Later on, when the confocal laser scanning microscope (CLSMs) became a commercially available and widespread instrument, spot-photobleaching was gradually replaced by photobleaching with a scanning laser beam (1,10,11,22,24,34–43). FRAP is currently a widely used technique because most commercial CLSMs nowadays are equipped with the feature to photobleach arbitrary user-defined areas. However, not so many easy to use and truly quantitative models exist for the analysis of FRAP experiments with a scanning laser beam. To address this need, we have recently reported a truly quantitative FRAP method and model that can be easily used with a CLSM (1). It is based on the uniform photobleaching of a circular area and can be used to study diffusion in three-dimensional (3-D) samples. Although the disk FRAP method yields very accurate diffusion measurements, the uniform photobleaching condition requires a disk radius of at least 5× times the resolution of the photobleaching beam. While this is not a problem for diffusion measurements in extended samples such as extracellular matrices or pharmaceutical solutions and gel systems, it is not optimal for measurements in small objects such as cells.

Here we report a new truly quantitative FRAP method and model that uses a very small bleach area. The new FRAP method can be carried out with a standard CLSM. The smallest bleach area that can be obtained with a scanning beam is a single line. We have, therefore, derived the exact physical solution to the problem of diffusion in a line photobleached by a focused scanning laser beam and imaged by a CLSM. The mathematical analysis leads to an analytical solution that can be easily programmed in a fitting routine for

Submitted October 21, 2006, and accepted for publication November 28, 2006.

Address reprint requests to Stefaan C. De Smedt, E-mail: stefaan.desmedt@ugent.be.

0006-3495/07/03/2172/12 $2.00

doi: 10.1529/biophysj.106.099838

the quantitative analysis of the recovery curves. First we will give an outline of the mathematical derivation that leads to the final analytical solution. The assumptions that were made in the derivation and their implications on the experiments will be discussed as well. We will test the influence of noise, confocal aperture, and bleaching power separately to assess the instrumental settings that are needed for optimal results. The ability of this ''line-FRAP'' method to accurately measure absolute diffusion coefficients and mobile fractions in 3-D samples will be evaluated in detail. Finally, an example experiment will be presented in which the line FRAP method is used to measure the diffusion coefficient of free green fluorescent protein (GFP) in the cytosol and nucleus of living A549 cells.

THEORY

Photobleaching of a long line segment

In almost all FRAP models the assumption is made that the photobleaching process can be described by first-order reaction kinetics (1,11,28,31,33,36,38,44–46). We have recently shown that this is not necessarily the case for the high-power photobleaching phase in a FRAP experiment (2). However, we have also shown that first-order reaction kinetics can still be used in the mathematical derivation as long as the resolution of the bleaching beam (focused by the microscope objective lens) is not a fixed value but a variable that changes as a function of laser power. We will therefore assume first-order photobleaching kinetics here and keep in mind that the resolution of the bleaching beam r_{0e} is a variable parameter. In the experimental section we will discuss how r_{0e} can be determined for a particular FRAP experiment.

We have shown before (1) that the fluorophore concentration after bleaching, $C_b(x, y, z)$, of a single line segment of length l (see Fig. 1) along the x axis can be calculated from:

$$C_b(x, y, z, T) = C_0(x, y, z)e^{-\frac{\alpha}{v}K(x,y,z)}, \quad (1)$$

where

$$K(x, y, z) = \int_{-l/2}^{l/2} L(x')I_b(x - x', y, z)dx', \quad (2)$$

and α is the photobleaching rate of the fluorophore, v the scanning speed of the bleaching laser beam, and $L(x)$ is the function that describes the modulation of the bleaching laser intensity along the line segment $[-l/2, l/2]$ and has values between 0 and 1, where 0 means light switched off and 1 means maximum bleaching intensity. During the bleaching phase of a FRAP experiment, the bleaching intensity remains constant: $L(x) = 1$. We will further assume to be working with low numerical aperture (NA) lenses with a virtual cylindrical beam profile and a Gaussian radial intensity distribution:

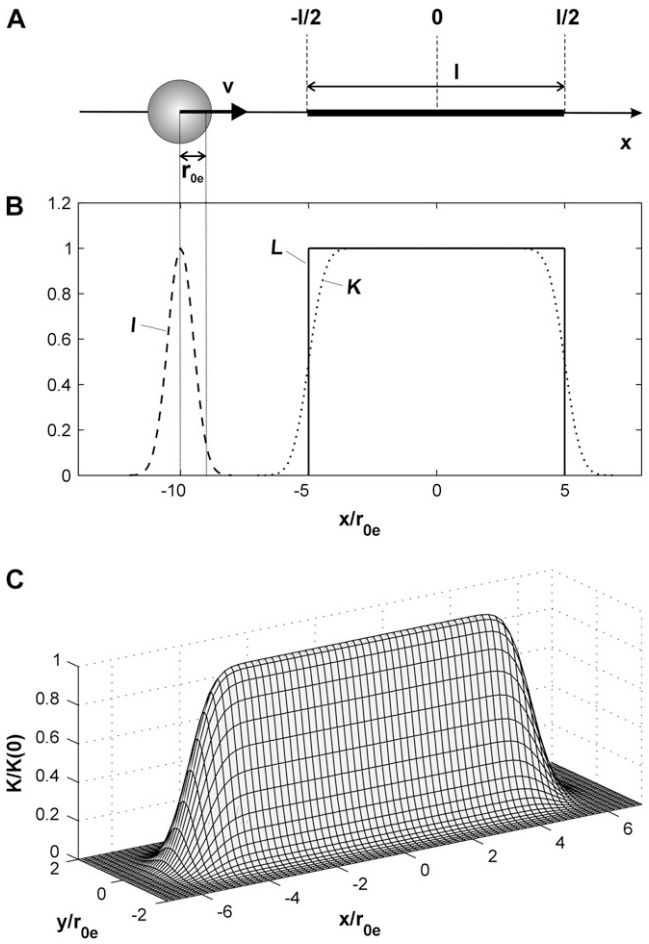

FIGURE 1 (*A*) A focused laser beam with effective resolution r_{0e} is scanned along the x-direction with speed v. From position $x = -l/2$ to $+l/2$ the laser intensity will be increased to photobleach a line segment of length l. The length of the line segment is $10 \times r_{0e}$ in this example. (*B*) The laser beam has a Gaussian radial intensity distribution I with resolution r_{0e} according to Eq. 3. The function L describes the modulation of the laser intensity and is 1 for $x \in [-l/2, l/2]$ and 0 anywhere else. According to Eq. 2, the convolution of I with L leads to the effective intensity distribution K for bleaching of the line segment. (*C*) Surface plot of the 2-D function $K(x,y)$ as calculated from Eq. 4. K is uniform along x ''far from the edges'' and has a Gaussian profile along y according to Eq. 5.

$$I_b(x, y, z) = I_{0b}e^{-2\frac{x^2+y^2}{r_{0e}^2}}. \quad (3)$$

We make the assumption of a low NA lens because we want to apply the FRAP method to 3-D samples. The use of low NA lenses avoids a significant contribution to the recovery from diffusion along the z axis (1,33) and reduces the complexity of the mathematical problem further on. In the experimental part we will discuss the conditions for which this assumption is valid. Note that, if one is working with thin two-dimensional (2-D) samples, Eq. 3 is valid for an objective lens of any NA. Combining Eqs. 2 and 3 leads to:

$$K(x,y,z) = \sqrt{\frac{\pi}{8}} I_{0b} r_{0e} \left(erf\left(\sqrt{2}\frac{x + l/2}{r_{0e}} \right) - erf\left(\sqrt{2}\frac{x - l/2}{r_{0e}} \right) \right) \times e^{-2\frac{y^2}{r_{0e}^2}}, \quad (4)$$

where *erf* is the well-known error function (see Fig. 1 *C*). To allow us to find an analytical solution to the FRAP model, we will now make the assumption of the bleached line segment being much longer than the resolution of the bleaching beam, i.e., $l \gg r_{0e}$. Then, at sufficient distance from both ends, i.e., $-l/2 \ll x \ll l/2$, Eq. 4 reduces to:

$$K(x,y,z) = \sqrt{\frac{\pi}{2}} I_{0b} r_{0e} e^{-2\frac{y^2}{r_{0e}^2}}. \quad (5)$$

The last assumption implies that the fluorescence recovery will have to be analyzed at sufficient distance from the ends of the bleached line segment to avoid a contribution from diffusion along the *x*-direction. Combining Eqs. 1 and 5, we finally find that the fluorophore concentration after bleaching of a long line segment can be calculated from:

$$C_b(x,y,z) = C_0(x,y,z) e^{-K_0 e^{-2\frac{y^2}{r_{0e}^2}}}, \quad (6)$$

where $K_0 = \sqrt{\frac{\pi}{2}} r_{0e} I_{0b} \frac{\alpha}{\gamma}$ is called the bleaching parameter because it determines directly the amount of bleaching.

Fluorescence recovery after photobleaching of a long line segment

After the photobleaching of the line segment, the bleached fluorophore molecules will be replaced by intact fluorophores by diffusion. The fluorophore concentration distribution at a time *t* after photobleaching can be calculated by solving Fick's second law (47):

$$\frac{\partial}{\partial^2 t} C(y,t) = D \frac{\partial}{\partial^2 y} C(y,t), \quad (7)$$

for the initial condition Eq. 6. *D* is the diffusion coefficient. The diffusion equation can be solved by applying a Fourier transform to the *y*-coordinate, finally leading to:

$$C(y,t) = C_0 \sum_{n=0}^{+\infty} \frac{(-K_0)^n}{n!} (a_n - n)^{-1/2} e^{-\frac{2ny^2}{(a_n - n) r_{0e}^2}}, \quad (8)$$

where $a_n = 1 + n(1 + 2t/\tau_r)$ and the characteristic recovery time $\tau_r = r_{0e}^2/4D$.

The fluorescence *F* as observed by a CLSM is calculated from the convolution product of the fluorophore concentration distribution *C* and the confocal PSF $I_c = I_{0c} e^{-2\frac{x^2+y^2}{r_{0c}^2}} e^{-2\frac{z^2}{z_{0c}^2}}$:

$$F(y,t) = q \int_{-\infty}^{+\infty} \int_{-\infty}^{+\infty} \int_{-\infty}^{+\infty} I_c(x',y',z') \times C(y' - y, t) dx' dy' dz', \quad (9)$$

where *q* is a constant factor taking all relevant quantum efficiencies and attenuation factors into account. Combining Eqs. 8 and 9 with the confocal PSF finally leads to:

$$\frac{F(y,t)}{F_0} = \sum_{n=0}^{+\infty} \frac{(-K_0)^n}{n!} r_{0e} (n r_{0c}^2 + (a_n - n) r_{0e}^2)^{-1/2} e^{-\frac{2ny^2}{n r_{0c}^2 + (a_n - n) r_{0e}^2}}, \quad (10)$$

where F_0 is the observed fluorescence before bleaching. To take an additional mobile fraction *k* into account, Eq. 10 has to be substituted into the right-hand side of

$$F(y,t) = F(y,0) + k(F(y,t) - F(y,0)), \quad (11)$$

where $F(y,0)$ is the fluorescence at $t = 0$, which is immediately after photobleaching.

It is worth recalling the assumptions we have made in the derivation of the line FRAP model that are to be met by the experimental conditions:

1. The fluorescent molecules in the sample have to be initially uniformly distributed. This means that there should be no concentration gradient present before bleaching that gives rise to net diffusion.
2. The diffusion process takes place in an infinite medium. This means that during the time period over which the recovery is observed, the diffusion front should not have reached any boundaries at which it will be reflected and influence the free diffusion process (47). By examining the sample with the confocal microscope, the user can choose an area that fulfills these requirements.
3. An objective lens of low NA should be used for bleaching and observation of the fluorescence recovery in a 3-D sample. Lenses of high NA can be used as well in combination with ''thin'' samples as long as: a), the bleaching profile along the axial direction stretches throughout the entire sample to avoid diffusion along the axial direction; and b), the part of the bleaching intensity distribution inside the sample is nearly cylindrical, which implies that, the higher the NA, the smaller the sample's thickness will have to be.
4. The fluorescence recovery should be analyzed sufficiently far from the start and end point of the bleach line.
5. The bleaching phase has to be sufficiently short to avoid recovery during bleaching.
6. Finally, there should be no flow present in the medium that can contribute to the fluorescence recovery.

MATERIALS AND METHODS

FRAP equipment

The FRAP experiments were performed on a CLSM (model MRC1024 UV, Bio-Rad, Hemel Hempstead, UK) modified to be able to bleach arbitrary regions (35) and equipped with a 4 W Ar-ion laser (model Stabilite 2017; Spectra-Physics, Darmstadt, Germany). A 10× objective lens (CFI Plan Apochromat; Nikon, Badhoevedorp, The Netherlands) with an NA of 0.45 was used. On the Bio-Rad MRC1024, however, the back aperture of this

lens is only partially filled, resulting in a lower effective NA and an increased resolution radius of $r_0 = 1.0$ μm. The power of the laser light coming out of the objective lens was measured with a laser power meter (Ophir, Wilmington, MA).

Test solutions

Two different fluorophores have been used for the evaluation of the line FRAP model: R-phycoerythrin (Molecular Probes, Leiden, The Netherlands) and fluorescein isothiocyanate dextrans (FITC-dextrans) (Sigma-Aldrich, Bornem, Belgium) of different molecular weights (FD2000: $M = 2\times10^6$ g/mol, FD464: $M = 4.64\times10^5$ g/mol, FD167: $M = 1.67\times10^5$ g/mol, FD71: $M = 71.6\times10^3$ g/mol). R-phycoerythrin was supplied as a suspension of 4 mg/ml in 60% saturated ammonium sulfate and 50 mM potassium phosphate, pH 7.0. Following the supplier's instructions, the suspension was centrifuged at 5000 rpm for 10 min, after which the pellet was dissolved in PBS buffer, pH 7.4. This suspension was brought into a semipermeable membrane and dialyzed against the same buffer for 24 h. The final suspension volume in the membrane was ~1.8 ml and was further diluted by adding PBS buffer to obtain a final concentration of ~1 mg/ml.

Before performing FRAP measurements on solutions of fluorescent molecules, the concentration range has to be determined in which a linear relation exists between the observed fluorescence and the concentration of the fluorescent molecule. Based on the outcome of such experiments, the following concentrations have been chosen: 1 mg/ml for R-phycoerythrin, 10 mg/ml for FD2000, 2 mg/ml for FD464, 6 mg/ml for FD167, and 6 mg/ml FD71. Next, solutions of the fluorescent molecules were prepared in HEPES buffer containing varying amounts of sucrose. The sucrose was used to vary the viscosity of the solutions and hence the diffusion coefficient of the fluorescent molecules.

To perform FRAP experiments, the fluorescent solutions were ''sandwiched'' between a microscope slide and a coverslip sealed by an adhesive spacer of 120 μm thickness (Secure-Seal Spacer; Molecular Probes) in between. Such a microscopic chamber is small enough to eliminate any currents in the solution while retaining a 3-D sample environment. The 496.5-nm line of the Ar-ion laser was used for excitation of R-phycoerythrin and the 488-nm line for the FITC-dextrans.

Cells

To generate GFP expressing cells, A549 cells were injected in the nucleus with a GFP encoding plasmid and incubated overnight. The gWIZ GFP encoding plasmid (5799 bp) was purchased from Gene Therapy Systems (San Diego, CA). A549 cells (African green monkey kidney cells, ATCC No. CCL-81) were cultured in DMEM without phenol red (Gibco, Merelbeke, Belgium) containing 2 mM glutamine, 10% heat deactivated fetal bovine serum (FBS), and 1% penicillin-streptomycin (culture medium) at 37°C in a humidified atmosphere containing 5% CO_2. A549 cells were grown to 80% confluence on glass-bottomed coverslips (part No. PG-1.5-14-F, glass bottom No. 1.5, MatTek, Ashland, MA) and injected in the nucleus using 1 μg/ml plasmid DNA in water. Microinjection was performed with a Femtojet microinjector and an Injectman NI 2 micromanipulator (Eppendorf, Hamburg, Germany). Subsequently, the cells were incubated overnight to allow for GFP expression.

Experimental FRAP protocol

The line FRAP method presented here can be carried out in two different ways, as can be seen from Eq. 10. First it is possible to record confocal *xy*-images of the fluorescence recovery after photobleaching of the line segment. From each of the *xy* recovery images, the fluorescence intensity profile along *y* (perpendicular to the bleach line) can be extracted and fitted directly by Eq. 10 to obtain the diffusion coefficient D. Although this method is the most accurate one since the entire fluorescence distribution is used to calculate D, its use in actual practice is limited because of the usually limited frame rates of CLSMs. This means that a CLSM will generally not be fast enough to image the recovery process at a sufficient sampling rate. Instead it will be much more likely to use the CLSM in *xt*-mode, where the laser beam is scanned repeatedly along a single line. The image that results from an *xt*-experiment consists of the same line that is displayed over time, as illustrated in Fig. 2. The FRAP protocol in *xt*-mode consists of the following sequential steps:

1. Record a number of line-scans at a low intensity to obtain the prebleach fluorescence signal F_0.
2. Activate the bleaching protocol to bleach a long line segment. The bleaching of the line segment may be repeated a number of times to increase the amount of bleaching. However, the overall bleach time should be small enough to avoid any significant recovery during bleaching.
3. Record the fluorescence recovery by continuing the *xt*-scan at a low intensity.

This method has the advantage of the recovery process being sampled at the CLSMs line-scanning rate (488 Hz for the CLSM of this study). It has the disadvantage that information from only a part of the bleach area is used. It also has the disadvantage that possible movement or flow in the sample cannot be easily detected, which could be an issue for very slow diffusion with long recovery times. The expression that should be used for fitting the recovery curve from an *xt*-experiment is Eq. 10 for $y = 0$:

$$\frac{F(0,t)}{F_0} = \sum_{n=0}^{+\infty} \frac{(-K_0)^n}{n!} r_{0e}\left(n r_{0c}^2 + (a_n - n) r_{0e}^2\right)^{-1/2}. \qquad (12)$$

On the CLSM, the sample is at first positioned on the microscope stage and the location of interest is brought into focus. As will be shown in the experimental section, the confocal diaphragm should be set to a small value to obtain correct results. For the 10× objective lens used in this study on the Bio-Rad MRC1024, the iris should be set to ≤1.5. The CLSM is set to *xt*-mode and a suitable zoom setting is chosen. Next, the length of the bleach line is defined in the photobleaching software, as well as the number of prebleach lines and the number of times the bleaching scan should be repeated. Then, the FRAP experiment is started and the *xt*-images are recorded. Two examples of *xt*-FRAP images are shown in Fig. 3. On the Bio-Rad MRC1024, at ''normal'' scanning speed, the pixel dwell-time is 2.4 μs and the time period between two line-scans is 2.048 ms. The images usually consist of 512 × 512 pixels. In case of slow recovery, multiple postbleach *xt*-images may be recorded.

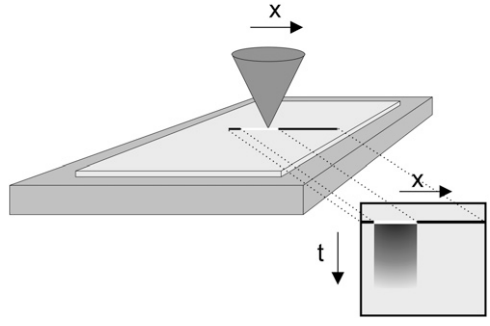

FIGURE 2 If the CLSM is working in *xt*-mode, the same line is scanned repeatedly, resulting in an *xt*-image consisting of the same line that is displayed over time. The *xt*-mode can be used for the line FRAP model. First a number of prebleach scans are recorded at a low laser intensity to determine the fluorescence intensity before bleaching. Next, a user-defined line segment is bleached at high laser intensity. Finally, the laser beam is switched back to its low intensity to record the fluorescence recovery after photobleaching.

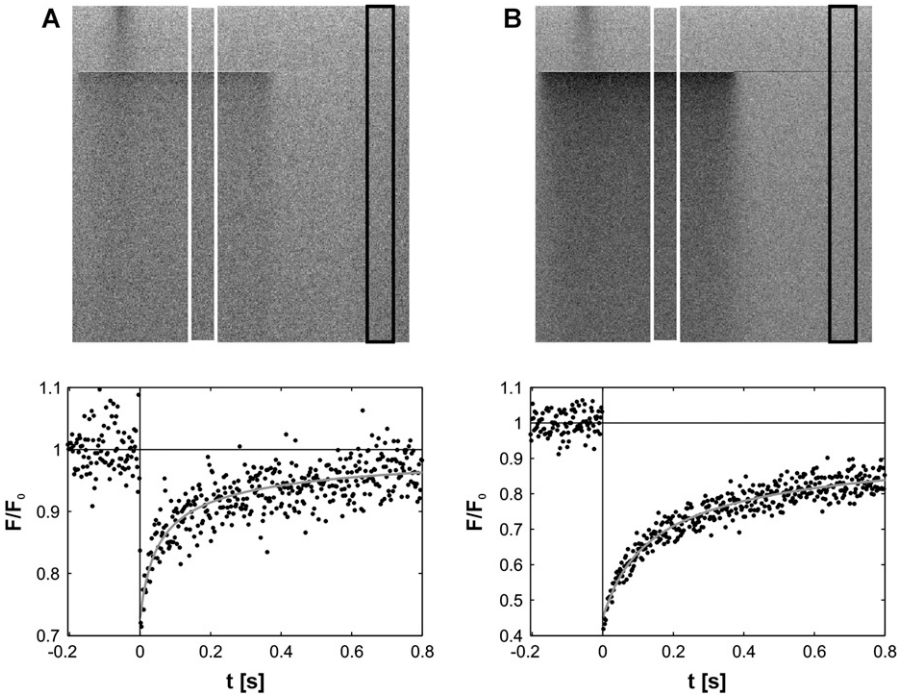

FIGURE 3 Two examples of *xt*-images are shown of a line FRAP experiment on a fluorescent solution (R-phycoerythrin with 36% (w/w) sucrose). First, 100 lines are recorded at a low laser intensity to determine the fluorescence before bleaching. Next, a line segment of 50 μm long is bleached with the 10× lens at 1 mW for image *A* and 4 mW for image *B*. After bleaching, the laser intensity is switched back to its previous (low) level to record the fluorescence recovery. As explained in the main text, the FRAP curve is extracted from the *xt*-images by defining a main ROI (*white rectangle*) and a background ROI (*black rectangle*). The final recovery curves (*black data points*) are shown below images *A* and *B*. The solid gray line shows the best fit of the line FRAP model to the experimental recovery curve. At the start of an image, the scanning beam of the Bio-Rad MRC1024 is stationary for a short period of time before actually starting the scanning movement. As a result, the fluorescence becomes bleached at the position where the laser beam is stationary. This is the reason why all *xt*-images have a bleach spot at the upper left corner that also recovers over time. This artifact causes the first 150 pixels of the images to be unusable. For that reason the main ROI is chosen toward the right end of the bleach line rather than at the center.

Data analysis

An image processing program was written to extract the experimental recovery curve from the *xt*-images. As indicated by the white rectangle in Fig. 3, a rectangular region of interest (ROI) can be defined of a certain length and width to calculate the fluorescence intensity as a function of time. The width of the ROI determines the number of pixels over which the fluorescence signal will be averaged for each line in the image. To correct for possible laser intensity fluctuations or possible bleaching while imaging the fluorescence recovery, a reference background ROI (BG) can be chosen as well (*black rectangle* in Fig. 3). To obtain the final recovery curve, the following calculations are performed: first, the ROI fluorescence curve is normalized against the BG curve; next, the average prebleach fluorescence is calculated from the prebleach lines; and finally, the fluorescence curve is normalized to the prebleach fluorescence. We note that, as always, it is important to set the zero-level of the confocal detectors correctly: zero fluorescence should give zero intensity in the images. Two examples of such final FRAP recovery curves are shown in Fig. 3 as well. The experimental parameters are finally determined by a least-squares fit of Eqs. 11 and 12 to the experimental recovery curve, as is shown by the gray curves in Fig. 3.

RESULTS AND DISCUSSION

Influence of noise

Because there are three model parameters (D, k, and K_0) that are determined from a best fit of the line FRAP model to the experimental recovery curve, it is worth looking separately at the influence of noise on the accuracy of the measured diffusion coefficient D and mobile fraction k. Based on Eq. 12, a FRAP curve was calculated for $D = 10\ \mu m^2/s$, $k = 1$, and $K_0 = 0.25$ to which a certain percentage of normally distributed noise was added. This was repeated for 20× from which the average recovery curve was calculated to simulate an ROI of 20 pixels wide. A best fit of Eqs. 11 and 12 was subsequently performed to calculate D, k, and K_0. A fitting to the same curve was done for a fixed value of $k = 1$ as well to see if the accuracy to calculate D increases when the mobile fraction is known. The results are shown in Fig. 4 for noise levels of 1%, 5%, 10%, 15%, 20%, and 25%. The result for each noise level is the mean value of 10 simulations. The error bars are the corresponding standard deviations (SDs). The results for D and K_0 when k was a free fitting parameter are shown in Fig. 4, *A* and *B*. The result for D when k was held fixed to 1 is shown in Fig. 4 *C*. As could be expected, the SDs increase with increasing noise levels. It is worth noting that in all cases the correct value is found within the SD. Interestingly, the accuracy (in terms of the SD) of D is not much better when the mobile fraction is held fixed to its correct value in the fitting algorithm. We therefore conclude that in the fitting of the experimental recovery curves, the mobile fraction k can be one of the fitting parameters without affecting the accuracy to determine the diffusion coefficient D.

Influence of the confocal aperture

In the derivation of the line FRAP model, we made the assumption of a cylindrical bleaching beam whose intensity distribution does not change along the optical axis. In 3-D samples, this situation will be best approximated by a low

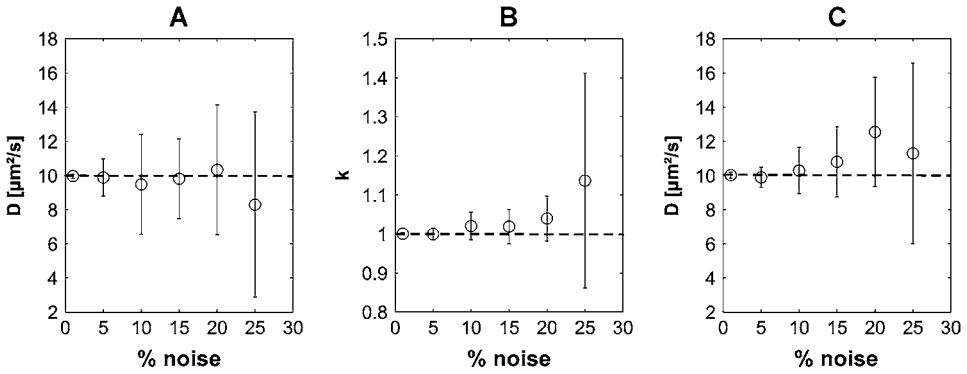

FIGURE 4 A recovery curve is simulated according to Eq. 12 for $D = 10$ $\mu m^2/s$, $k = 1$, and $K_0 = 0.25$ to which different percentages of normally distributed noise is added. To evaluate the influence of noise on the measured parameters, a fit of Eqs. 11 and 12 is subsequently applied to these data. The average value of 10 simulations is calculated for each noise level. The results for the diffusion coefficient D when the mobile fraction k is one of the free fitting parameters are shown in panel *A*. The corresponding result for the mobile fraction k is shown in panel *B*. The results for the diffusion coefficient D when the mobile fraction k is held fixed to its correct value of 1 is shown in panel *C*. The error flags are the mean ± SD values. Although the SDs increase for increasing noise levels, the correct value is found in all cases within the SD. Comparing the results from panel *A* with panel *C* shows that the diffusion coefficient is not more accurately determined when k is held fixed in the fittings.

NA lens. In reality, however, the illumination intensity distribution is not perfectly cylindrical, but has a slight conical shape. This means that the illumination beam becomes wider at larger distances from the focal plane. Therefore, when bleaching a single line, the width of the line will also gradually increase at increasing distance from the focal plane. The fluorescence recovery after bleaching will be different along the optical axis as well because it depends directly on the width (squared!) of the line (cfr. Eq. 10). When imaging with a large confocal aperture, the detected fluorescence recovery will therefore be an average of the recoveries at the different planes along the optical axis. When fitting the recovery curve with Eq. 12, it is therefore to be expected that the measured diffusion coefficient will be lower than the actual value for large confocal apertures. At the other hand, for a small confocal aperture the detected fluorescence will come mainly from the cylindrical region around the focal plane (see Fig. 5) and it is to be expected that the diffusion coefficient will be measured correctly.

To determine the influence of the confocal aperture on the measured diffusion coefficient, we have performed FRAP experiments on R-phycoerythrin (dissolved in a 36% (w/w) sucrose solution) for different settings of the confocal aperture. The results are shown in Fig. 6 *A* where the measured diffusion coefficient is plotted as a function of the confocal aperture setting of the CLSM. Each value of D is the mean value of 10 measurements. The error bars are the corresponding SDs. Bleaching was done at 500 μW (laser power coming out of the objective lens). A value of 1.25 μm for r_{0e} was used in the fittings, which is a correct value for R-phycoerythrin at this bleaching intensity as will be shown further on. As expected, the measured diffusion coefficient decreases for large confocal apertures. Within the experimental accuracy, no difference is found for D at iris settings smaller than 2. The diffusion coefficient of the same solution was measured with a disk FRAP model (1) as well, yielding $D = 11.83 \pm 0.49$ $\mu m^2/s$. This is indicated in Fig. 6 *A* by the horizontal lines. Indeed a good correspondence is found with the values measured with the line FRAP model at iris settings smaller than 2. For the objective lens used here (10×, NA 0.45) on the Bio-Rad MRC1024, an iris setting of 2 means a pinhole size of ~2.5 airy units (the other iris settings scale linearly). We note that the results from Fig. 6 depend on the effective NA of the objective lens being used for photobleaching, which determines how ''cylindrical'' the bleaching beam is (see Fig. 5). This experiment has to be repeated for a particular objective lens to determine the correct maximum confocal diaphragm setting.

The same experiment was repeated on FD167 (dissolved in a 20% (w/w) sucrose solution). Bleaching was done at 2000 μW. A value of 2.1 μm was taken for r_{0e}, which is a correct value for FD167 at this bleaching intensity, as will be shown further on. The results are shown in Fig. 6 *B*. In agreement with the results for R-phycoerythrin, we find that D is independent of the confocal aperture for iris settings smaller than 2. The diffusion coefficient obtained with the

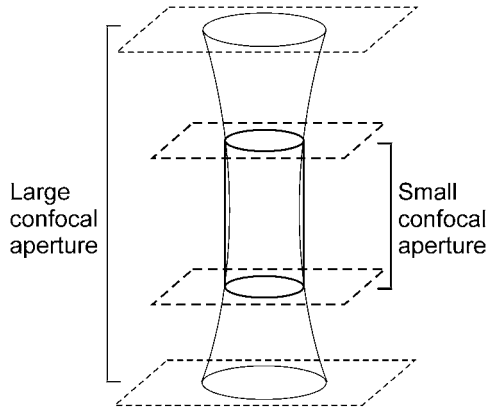

FIGURE 5 Even for low NA lenses, the focused beam profile is not perfectly cylindrical, but has a slight conical shape. To comply with the assumption of a cylindrical bleaching beam, the fluorescence recovery should therefore be imaged with a small confocal aperture to record information of the cylindrical region near the focal plane alone.

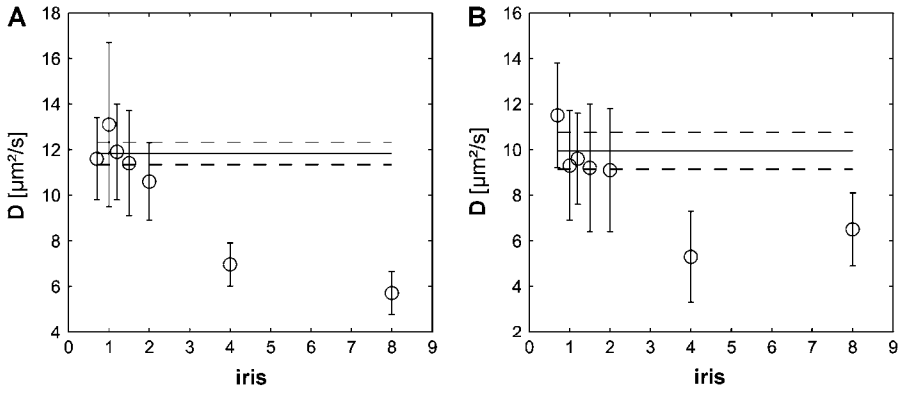

FIGURE 6 FRAP experiments were performed for varying confocal iris settings on (*A*) a solution of R-phycoerythrin (in 36% (w/w) sucrose) and (*B*) a solution of FD167 (in 20% (w/w) sucrose). Each value for D is the mean of 10 measurements. The error bars are the corresponding mean ± SDs. The diffusion coefficient of the same solutions was measured by the disk FRAP model as well, as indicated by the horizontal solid line. The dashed lines indicate the corresponding SD value.

disk FRAP model was $D = 9.95 \pm 0.80\ \mu m^2/s$. Again there is a good correspondence with the line FRAP model if the iris is set at a value smaller than 2.

Influence of the bleaching power

We have recently shown that the effective resolution r_{0e} of the bleaching beam depends on the bleaching power (2). For this very reason, an independent bleaching and imaging resolution, respectively, r_{0e} and r_{0c}, was taken into account in the derivation of the line FRAP model. We will now examine directly the influence of the bleaching power P on the effective bleaching resolution r_{0e} for both R-phycoerythrin and FD167. This can be done by performing line FRAP experiments for different bleaching powers on a solution of a known diffusion coefficient. The effective bleaching resolution r_{0e} can be determined by fitting of the recovery curves with Eq. 12 for a known value of D.

First, the diffusion coefficient of a solution of R-phycoerythrin (in 36% (w/w) sucrose) was measured with the disk FRAP model: $D = 11.83 \pm 0.49\ \mu m^2/s$. Next, line FRAP experiments were performed on the same solution for different bleaching powers ranging from 0.32 to 4 mW (laser power coming out of the objective lens). The results for the effective bleaching resolution r_{0e} measured as a function of the laser power are shown in Fig. 7 *A*, where each value is the mean of 10 measurements. The error bars are the corresponding SDs. These results support directly our previous results (2): the effective bleaching resolution increases with increasing bleaching power. For low bleaching powers, r_{0e} approaches a value of 1 μm, which is the real resolution of the illumination intensity distribution. Because the experimental accuracy decreases for lower bleaching powers, we suggest using a power between 0.5 and 1 mW for bleaching of R-phycoerythrin and an r_{0e} value of 1.25 μm.

The same experiment was repeated on FD167 (in 20% (w/w) sucrose). A diffusion coefficient of $D = 9.95 \pm 0.80\ \mu m^2/s$ was found with the disk FRAP model. Line FRAP experiments were performed on the same solution for bleaching powers between 1 and 5 mW. We note at this instance that fluorescein photobleaches less easily compared to R-phycoerythrin. Therefore it was not possible to obtain sufficient bleaching for powers below 1 mW. The results are shown in Fig. 7 *B*. Each value is again the mean of 10 measurements and the error bars are the corresponding SDs. Again we find an increasing bleaching resolution with increasing bleaching power. For FITC-dextrans we suggest using a bleaching power between 1 and 2 mW with an r_{0e} value of 2.1 μm for the 10× objective lens used here.

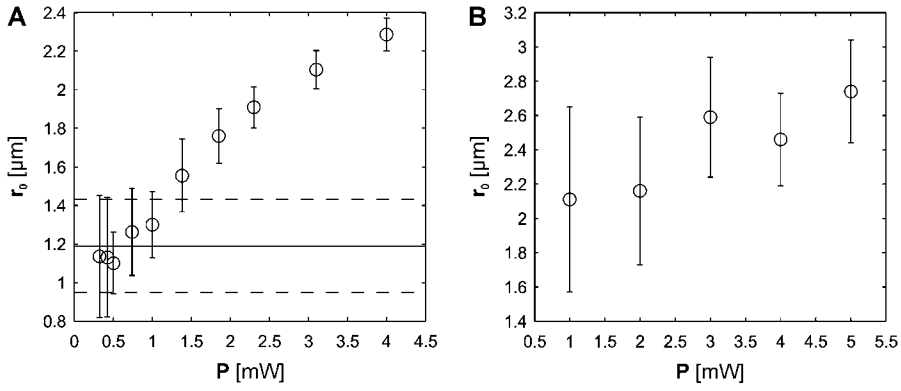

FIGURE 7 Line FRAP experiments were performed for different bleaching powers on (*A*) a solution of R-phycoerythrin (in 36% (w/w) sucrose) and (*B*) a solution of FD167 (in 20% (w/w) sucrose). The effective bleaching resolution radius was determined by fitting of the line FRAP model to the recovery curves. Each value for r_{0e} is the mean of 10 measurements. The error bars are the corresponding SDs. The horizontal line in panel *A* indicates the mean of all r_{0e} values that correspond to a bleaching power ≤1 mW. The dashed lines indicate the corresponding mean ± SD levels.

Validation of the line FRAP model

Having found the correct settings for the confocal aperture and the bleaching power, the ability of the line FRAP model to accurately measure absolute diffusion coefficients can now be evaluated. This can be done by comparing the diffusion coefficient as determined from line FRAP experiments with the diffusion coefficient obtained with the disk FRAP model. This is a valid approach because the disk FRAP model has already been proven to be able to accurately measure absolute diffusion coefficients (1).

R-phycoerythrin solutions were prepared, containing different concentrations of sucrose (30, 36, 40, 44, 48, and 56% w/w), to obtain a range of diffusion coefficients. The diffusion coefficient of R-Phycoerythrin in each of the solutions was measured with both the disk and line FRAP method. The bleaching power was always 1 mW (laser power coming out of the objective lens) and a corresponding bleaching resolution r_{0e} of 1.25 μm was used to calculate the diffusion coefficients. In Fig. 8, the diffusion coefficients measured with the line FRAP model are plotted against the diffusion coefficients measured with the disk FRAP model. Ideally, the data points should be spread along the diagonal, which is the case within the experimental error. A *t*-test (for distributions with unequal standard deviation and a significance level of 0.01) on each data pair also confirmed that both methods yield the same results.

The same experiments were repeated for four FITC-dextrans, each dissolved in a series of solutions with different concentrations of sucrose. The bleaching power was 2 mW and a corresponding bleaching resolution r_{0e} of 2.1 μm was used to calculate the diffusion coefficients. The results for all FITC-dextrans are shown in Fig. 9 where the diffusion coefficient obtained with the line FRAP model is plotted against the diffusion coefficient obtained with the disk FRAP model. Again we found a good correspondence between the line and disk FRAP model within the experimental accuracy (additionally confirmed by a *t*-test on each data pair). We note that the apparent increasing deviation from the solid lines in Fig. 9 for increasing *D*-values is because of the increase in absolute values. There is no particular tendency in magnitude of the relative deviation between the results from the disk and line FRAP methods.

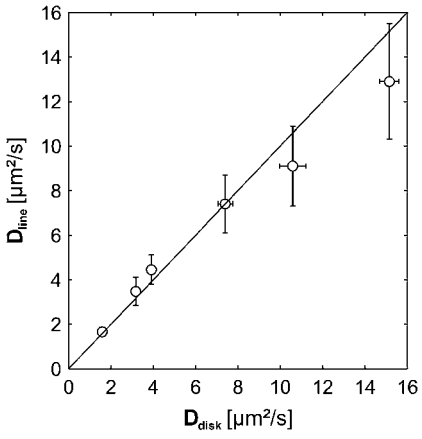

FIGURE 8 The diffusion coefficient of R-phycoerythrin in solutions of different viscosity is measured with both the disk (five measurements for each sample) and line FRAP method (10 measurements for each sample). The diffusion coefficients measured with the line FRAP model are in good agreement with the values from the disk FRAP model within the experimental accuracy.

These experiments show that absolute diffusion coefficients can be measured correctly in 3-D samples with the line FRAP model on condition that the effective bleaching resolution is known and the confocal aperture is correctly set. The experiments also show that, within the experimental error, it is sufficient to determine the effective bleaching resolution from a single solution (although there might be a small change in reality because of the difference in viscosity and refractive index). By comparing the SD values of the disk FRAP model with the SD values of the line FRAP model it is clear that, as expected, the accuracy of the disk FRAP model is superior to the line FRAP model. While the relative SD error of *D* measured with the disk FRAP model is typically around 5%, it is rather 20–25% for the line FRAP model. We have observed that the same holds true for the mobile fraction: the mobile fraction is measured correctly with the line FRAP model, but with a reduced accuracy as compared to the disk FRAP model. At the other hand, the line FRAP method is much faster than the disk FRAP method because it uses a much smaller bleach area. For the same reason the line FRAP method can perform much more localized diffusion measurements as well. We conclude that both FRAP methods are complementary, each with their own benefits and limitations. One of both methods can be used depending on the problem at hand.

The highest diffusion coefficient that can be reasonably measured with a FRAP method can be estimated based on the characteristic recovery time (see Eq. 8). Because the disk FRAP recovery curves usually have very little noise (signal integrated over many pixels), it is our experience that one measurement before the characteristic time point is sufficient to calculate a correct diffusion coefficient. The rate at which data points can be obtained depends on the maximum frame rate of the confocal microscope. On the Bio-Rad 1024 used in this study, the maximum frame rate is approx. 1.5 s per image. This means that the characteristic recovery time should be at least 3 s. If one uses a disk of radius 20 μm this comes down to a maximum diffusion coefficient of $\sim$30 $\mu m^2/s$. Newer confocal systems can have frame rates of 0.5 s per image (or less), which would give a maximum diffusion coefficient of $\sim$100 $\mu m^2/s$. In addition, increasing the size of the disk allows one to measure even faster diffusion. The size of the bleach area in case of the line FRAP method is determined by the effective bleaching resolution (which is a function of the objective lens, the fluorophore, and photobleaching laser power). For the objective lens of this study and not too high

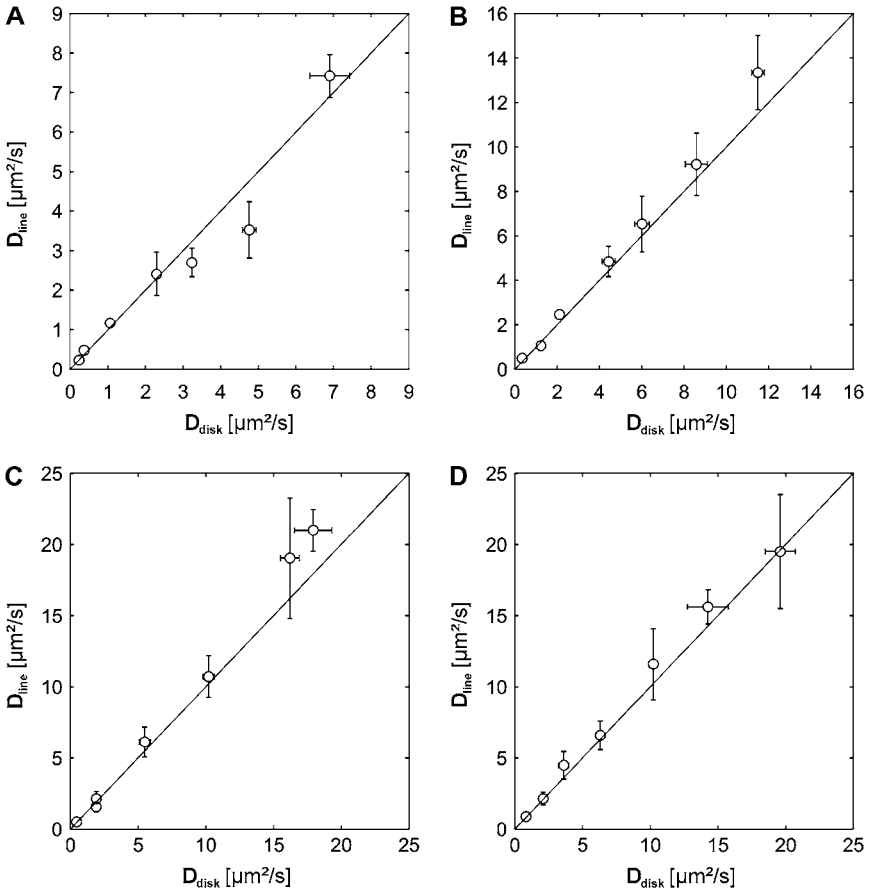

FIGURE 9 The diffusion coefficients of four types of FITC-dextran in solutions of different viscosities is measured with both the disk and line FRAP method: (*A*) FD2000, (*B*) FD464, (*C*) FD167, and (*D*) FD71. The diffusion coefficients measured with the line FRAP model (10 measurements for each sample) are in good agreement with the values from the disk FRAP model (five measurements for each sample) within the experimental accuracy.

bleach powers we found an effective bleaching resolution of 1.25 μm for R-phycoerythrin. Because of the higher noise level, one rather needs ~10 data points before the characteristic time point. Since the line-scan rate is ~2 ms on our Bio-Rad confocal, the characteristic recovery time should be at least 20 ms, leading to a maximum diffusion coefficient of ~20 $\mu m^2/s$. Newer confocals can have line scan rates of 1 ms per line, increasing the maximum diffusion coefficient to 40 $\mu m^2/s$. For fluorescein the effective bleaching resolution was rather 2.1 μm, giving a maximum diffusion coefficient of 55 $\mu m^2/s$ (and ~100 $\mu m^2/s$ for newer confocals). We conclude that both the disk and line FRAP methods can reasonably measure diffusion coefficients up to ~100 $\mu m^2/s$ on new CLSMs, although it was limited to ~30 $\mu m^2/s$ on the Bio-Rad CLSM of this study.

APPLICATION TO INTRACELLULAR DIFFUSION MEASUREMENTS

By way of example, we show the application of the new line FRAP method to the measurement of free GFP diffusion in living A549 cells. A long line segment is bleached with the 10× objective lens across the cell interior, as indicated in Fig. 10 *A*. The resulting *xt*-image is shown in Fig. 10 *B*. Because the recovery is due to diffusion perpendicular to the bleached line, the user has the possibility to do the FRAP analysis in one or more subregions along the line segment. We have, therefore, done the analysis for two regions along the line, as indicated by the letters *a* (nucleus) and *b* (cytoplasm). The recovery curves from regions *a* and *b* are shown in Fig. 10, *C* and *D*. From six similar measurements we found a diffusion coefficient of 26 ± 3 $\mu m^2/s$ in the cytoplasm and 29 ± 5 $\mu m^2/s$ in the nucleus, in good agreement with what others have reported (5,8,48).

CONCLUSIONS

A new FRAP method has been presented based on the photobleaching of a line segment that is much longer than the effective resolution of the bleaching beam. By additionally excluding diffusion along the optical axis, the recovery process is reduced to a one-dimensional problem for which we have been able to find an analytical solution. We have shown that the latter condition is fulfilled for measurements in 3-D samples if the bleaching is done with a low NA objective lens in combination with a small confocal aperture. The line FRAP method is expected to work fine in combination with objective lenses of higher NA as well, if

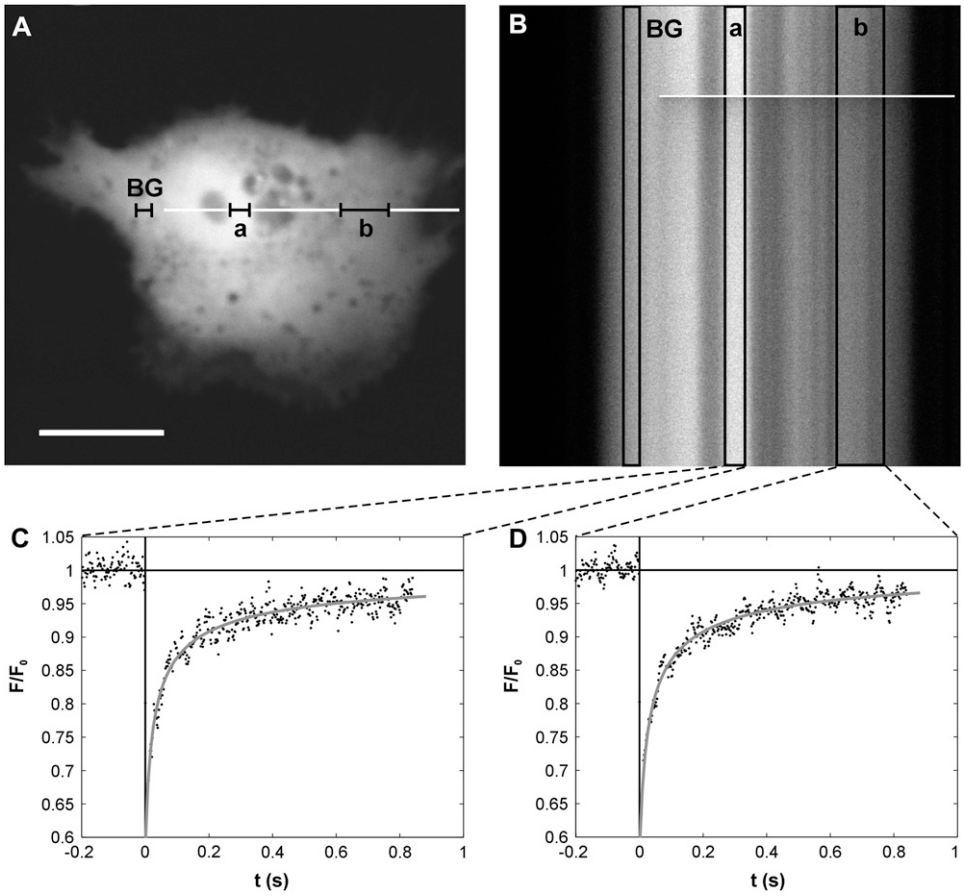

FIGURE 10 Application of the line FRAP method to a GFP expressing A549 cell. (*A*) The white line indicates the line segment that will be photobleached. Subregions *a* (nucleus) and *b* (cytoplasm) will be analyzed. Subregion BG is the background region that will be used in the calculation of the recovery curves. The scale bar is 20 μm. (*B*) *xt*-image showing the line FRAP experiment. First 100 prebleach scans are recorded. Next, a single bleach scan is performed followed by the recording of the fluorescence recovery. (*C*) The recovery curve as calculated from subregion *a* (nucleus) together with a best fit (*gray line*) according to the line FRAP model. The diffusion coefficient calculated from this particular measurement is $D = 27.4\ \mu m^2/s$. (*D*) The recovery curve as calculated from subregion *b* (cytoplasm) together with a best fit (*gray line*) according to the line FRAP model. The diffusion coefficient calculated from this particular measurement is $D = 24.8\ \mu m^2/s$.

the sample is sufficiently thin to avoid side effects from the conical shape of the bleaching beam.

We have recently shown that the effective resolution of the bleaching beam depends strongly on the laser power being used for photobleaching (2). By incorporating an independent bleaching and imaging resolution into the line FRAP model, we were able to evaluate these findings quantitatively for actual solutions of fluorescent molecules. For R-phycoerythrin, a strong dependency was found of the effective bleaching resolution r_{0e} on the bleaching power P. A similar dependency of r_{0e} on P was found for FD167. We also found that the r_{0e} value, as determined from a single solution, is valid for all other solutions of the same fluorescent molecules, regardless of their viscosity (or molecular weight of the dextran chains in case of the FITC-dextrans).

We have shown that the line FRAP method is able to correctly measure absolute diffusion coefficients. Compared to the disk FRAP method, the line FRAP method has the disadvantage of being less accurate due to a lower signal/noise ratio. This is because the recovery signal is integrated from typically 20–40 pixels, whereas 1000–2000 pixels are used for the disk FRAP method. The line FRAP method has the advantage of using a smaller bleaching region, thus allowing more localized measurements. A related advantage is that the line FRAP method is much faster than the disk FRAP model because the characteristic diffusion time is proportional to the area of the bleach region. With the line FRAP method it is also possible to do diffusion measurements in different regions of the bleach line simultaneously. We have demonstrated this by the simultaneous measurement of the diffusion of free GFP in the cytoplasm and nucleus of A549 cells.

We conclude that the line FRAP model offers a straightforward and fast way to measure diffusion coefficients and mobile fractions on a microscopic scale in 3-D samples. Because the bleaching of a line can be easily accomplished by commercial CLSMs, it can be applied by anyone familiar with the CLSM instrument. Additionally, no extensive mathematical or programming skills are required because the final FRAP expressions are very straightforward.

We thank Bart Huyck for his help with carrying out the FRAP experiments.

The financial support of the IWT (Instituut voor de Aanmoediging van Innovatie door Wetenschap en Technologie in Vlaanderen) is acknowledged with gratitude. Ghent University (Bijzonder Onderzoeksfonds) is acknowledged for its support through instrumentation credits. Kevin Braeckmans is a Postdoctoral Fellow of the Fund for Scientific Research, Flanders (Belgium).

REFERENCES

1. Braeckmans, K., L. Peeters, N. N. Sanders, S. C. De Smedt, and J. Demeester. 2003. Three-dimensional fluorescence recovery after photobleaching with the confocal scanning laser microscope. *Biophys. J.* 85:2240–2252.
2. Braeckmans, K., B. Stubbe, K. Remaut, J. Demeester, and S. C. De Smedt. 2006. Anomalous photobleaching in fluorescence recovery after photobleaching measurements due to excitation saturation: a case study for fluorescein. *J. Biomed. Opt.* 11:044013.
3. Peters, R., J. Peters, K. H. Tews, and W. Bahr. 1974. Microfluorimetric study of translational diffusion in erythrocyte-membranes. *Biochim. Biophys. Acta.* 367:282–294.
4. Kao, H. P., J. R. Abney, and A. S. Verkman. 1993. Determinants of the translational mobility of a small solute in cell cytoplasm. *J. Cell Biol.* 120:175–184.
5. Seksek, O., J. Biwersi, and A. S. Verkman. 1997. Translational diffusion of macromolecule-sized solutes in cytoplasm and nucleus. *J. Cell Biol.* 138:131–142.
6. Lukacs, G. L., P. Haggie, O. Seksek, D. Lechardeur, N. Freedman, and A. S. Verkman. 2000. Size-dependent DNA mobility in cytoplasm and nucleus. *J. Biol. Chem.* 275:1625–1629.
7. Verkman, A. S. 2003. Diffusion in cells measured by fluorescence recovery after photobleaching. *In* Biophotonics, Part A: Methods in Enzymology. G. Marriott, and I. Parker, editors. Academic Press, New York. 635–648.
8. Elsner, M., H. Hashimoto, J. C. Simpson, D. Cassel, T. Nilsson, and M. Weiss. 2003. Spatiotemporal dynamics of the COPI vesicle machinery. *EMBO Rep.* 4:1000–1005.
9. Karpova, T. S., T. Y. Chen, B. L. Sprague, and J. G. McNally. 2004. Dynamic interactions of a transcription factor with DNA are accelerated by a chromatin remodeller. *EMBO Rep.* 5:1064–1070.
10. Braga, J., J. M. P. Desterro, and M. Carmo-Fonseca. 2004. Intracellular macromolecular mobility measured by fluorescence recovery after photobleaching with confocal laser scanning microscopes. *Mol. Biol. Cell.* 15:4749–4760.
11. Wedekind, P., U. Kubitscheck, O. Heinrich, and R. Peters. 1996. Line-scanning microphotolysis for diffraction-limited measurements of lateral diffusion. *Biophys. J.* 71:1621–1632.
12. Koppel, D. E. 1985. Normal-mode analysis of lateral diffusion on a bounded membrane surface. *Biophys. J.* 47:337–347.
13. Lippincott-Schwartz, J., J. F. Presley, K. J. M. Zaal, K. Hirschberg, C. D. Miller, and J. Ellenberg. 1999. Monitoring the dynamics and mobility of membrane proteins tagged with green fluorescent protein. *Methods Cell Biol.* 58:261–281.
14. Umenishi, F., J. M. Verbavatz, and A. S. Verkman. 2000. cAMP regulated membrane diffusion of a green fluorescent protein-aquaporin 2 chimera. *Biophys. J.* 78:1024–1035.
15. Chen, Y., B. C. Lagerholm, B. Yang, and K. Jacobson. 2006. Methods to measure the lateral diffusion of membrane lipids and proteins. *Methods.* 39:147–153.
16. Sanders, N. N., S. C. De Smedt, and J. Demeester. 2000. The physical properties of biogels and their permeability for macromolecular drugs and colloidal drug carriers. *J. Pharm. Sci.* 89: 835–849.
17. Olmsted, S. S., J. L. Padgett, A. I. Yudin, K. J. Whaley, T. R. Moench, and R. A. Cone. 2001. Diffusion of macromolecules and virus-like particles in human cervical mucus. *Biophys. J.* 81:1930–1937.
18. Pluen, A., Y. Boucher, S. Ramanujan, T. D. McKee, T. Gohongi, E. di Tomaso, E. B. Brown, Y. Izumi, R. B. Campbell, D. A. Berk, and R. K. Jain. 2001. Role of tumor-host interactions in interstitial diffusion of macromolecules: cranial vs. subcutaneous tumors. *Proc. Natl. Acad. Sci. USA.* 98:4628–4633.
19. Ramanujan, S., A. Pluen, T. D. McKee, E. B. Brown, Y. Boucher, and R. K. Jain. 2002. Diffusion and convection in collagen gels: implications for transport in the tumor interstitium. *Biophys. J.* 83: 1650–1660.
20. Peeters, L., N. N. Sanders, K. Braeckmans, K. Boussery, J. V. de Voorde, S. C. De Smedt, and J. Demeester. 2005. Vitreous: a barrier to nonviral ocular gene therapy. *Invest. Ophthalmol. Vis. Sci.* 46:3553–3561.
21. De Smedt, S. C., A. Lauwers, J. Demeester, Y. Engelborghs, G. Demey, and M. Du. 1994. Structural information on hyaluronic-acid solutions as studied by probe diffusion experiments. *Macromolecules.* 27:141–146.
22. De Smedt, S. C., T. K. L. Meyvis, J. Demeester, P. Van Oostveldt, J. C. G. Blonk, and W. E. Hennink. 1997. Diffusion of macromolecules in dextran methacrylate solutions and gels as studied by confocal scanning laser microscopy. *Macromolecules.* 30:4863–4870.
23. Meyvis, T. K. L., S. C. De Smedt, P. Van Oostveldt, and J. Demeester. 1999. Fluorescence recovery after photobleaching: a versatile tool for mobility and interaction measurements in pharmaceutical research. *Pharm. Res.* 16:1153–1162.
24. Burke, M. D., J. O. Park, M. Srinivasarao, and S. A. Khan. 2000. Diffusion of macromolecules in polymer solutions and gels: a laser scanning confocal microscopy study. *Macromolecules.* 33:7500–7507.
25. Ibarz, G., L. Dahne, E. Donath, and H. Mohwald. 2002. Controlled permeability of polyelectrolyte capsules via defined annealing. *Chem. Mater.* 14:4059–4062.
26. Van Tomme, S. R., B. G. De Geest, K. Braeckmans, S. C. De Smedt, F. Siepmann, J. Siepmann, C. F. van Nostrum, and W. E. Hennink. 2005. Mobility of model proteins in hydrogels composed of oppositely charged dextran microspheres studied by protein release and fluorescence recovery after photobleaching. *J. Controlled Release.* 110:67–78.
27. Alvarez-Mancenido, F., K. Braeckmans, S. C. De Smedt, J. Demeester, M. Landin, and R. Martinez-Pacheco. 2006. Characterization of diffusion of macromolecules in konjac glucomannan solutions and gels by fluorescence recovery after photobleaching technique. *Int. J. Pharm.* 316:37–46.
28. Axelrod, D., D. E. Koppel, J. Schlessinger, E. Elson, and W. W. Webb. 1976. Mobility measurement by analysis of fluorescence photobleaching recovery kinetics. *Biophys. J.* 16:1055–1069.
29. Koppel, D. E. 1979. Fluorescence redistribution after photobleaching: new multipoint analysis of membrane translational dynamics. *Biophys. J.* 28:281–291.
30. Yguerabide, J., J. A. Schmidt, and E. E. Yguerabide. 1982. Lateral mobility in membranes as detected by fluorescence recovery after photobleaching. *Biophys. J.* 40:69–75.
31. Soumpasis, D. M. 1983. Theoretical-analysis of fluorescence photobleaching recovery experiments. *Biophys. J.* 41:95–97.
32. Lopez, A., L. Dupou, A. Altibelli, J. Trotard, and J. F. Tocanne. 1988. Fluorescence recovery after photobleaching (FRAP) experiments under conditions of uniform disk illumination: critical comparison of analytical solutions, and a new mathematical method for calculation of diffusion coefficient-D. *Biophys. J.* 53:963–970.
33. Blonk, J. C. G., A. Don, H. Van Aalst, and J. J. Birmingham. 1993. Fluorescence photobleaching recovery in the confocal scanning light-microscope. *J. Microsc.* 169:363–374.
34. Kubitscheck, U., P. Wedekind, and R. Peters. 1994. Lateral diffusion measurement at high-spatial-resolution by scanning microphotolysis in a confocal microscope. *Biophys. J.* 67:948–956.
35. Wedekind, P., U. Kubitscheck, and R. Peters. 1994. Scanning microphotolysis: a new photobleaching technique based on fast intensity modulation of a scanned laser-beam and confocal imaging. *J. Microsc.* 176:23–33.
36. Cutts, L. S., P. A. Robberts, J. Adler, M. C. Davies, and C. D. Melia. 1995. Determination of localized diffusion-coefficients in gels using confocal scanning laser microscopy. *J. Microsc.* 180:131–139.
37. Kubitscheck, U., M. Tschodrich-Rotter, P. Wedekind, and R. Peters. 1996. Two-photon scanning microphotolysis for three-dimensional data storage and biological transport measurements. *J. Microsc.* 182: 225–233.
38. Kubitscheck, U., P. Wedekind, and R. Peters. 1998. Three-dimensional diffusion measurements by scanning microphotolysis. *J. Microsc.* 192: 126–138.

39. Peters, R., and U. Kubitscheck. 1999. Scanning microphotolysis: three-dimensional diffusion measurement and optical single-transporter recording. *Methods.* 18:508–517.

40. Gribbon, P., B. C. Heng, and T. E. Hardingham. 1999. The molecular basis of the solution properties of hyaluronan investigated by confocal fluorescence recovery after photobleaching. *Biophys. J.* 77: 2210–2216.

41. Brown, E. B., E. S. Wu, W. Zipfel, and W. W. Webb. 1999. Measurement of molecular diffusion in solution by multiphoton fluorescence photobleaching recovery. *Biophys. J.* 77:2837–2849.

42. Carrero, G., D. McDonald, E. Crawford, G. de Vries, and M. J. Hendzel. 2003. Using FRAP and mathematical modeling to determine the in vivo kinetics of nuclear proteins. *Methods.* 29:14–28.

43. Seiffert, S., and W. Oppermann. 2005. Systematic evaluation of FRAP experiments performed in a confocal laser scanning microscope. *J. Microsc.* 220:20–30.

44. Gordon, G. W., B. Chazotte, X. F. Wang, and B. Herman. 1995. Analysis of simulated and experimental fluorescence recovery after photobleaching: data for two diffusing components. *Biophys. J.* 68:766–778.

45. Feder, T. J., I. Brust-Mascher, J. P. Slattery, B. Baird, and W. W. Webb. 1996. Constrained diffusion or immobile fraction on cell surfaces: a new interpretation. *Biophys. J.* 70:2767–2773.

46. Dietrich, C., R. Merkel, and R. Tampe. 1997. Diffusion measurement of fluorescence-labeled amphiphilic molecules with a standard fluorescence microscope. *Biophys. J.* 72:1701–1710.

47. Crank, J. 1975. The Mathematics of Diffusion. Clarendon Press, Oxford, UK.

48. Maertens, G., J. Vercammen, Z. Debyser, and Y. Engelborghs. 2005. Measuring protein-protein interactions inside living cells using single color fluorescence correlation spectroscopy. Application to human immunodeficiency virus type I integrase and LEDGF/p75. *FASEB J.* 19:1039–1041.